

5 June 2000

# Glueballs: A central mystery

Frank E. Close<sup>1</sup>

*CERN, Geneva, Switzerland*

*and*

*Rutherford Appleton Laboratory*

*Chilton, Didcot, OX11 0QX, England*

## Abstract

Glueball candidates and  $q\bar{q}$  mesons have been found to be produced with different momentum and angular dependences in the central region of  $pp$  collisions. This talk illustrates this phenomenon and explains the  $\phi$  and  $t$  dependences of mesons with  $J^{PC} = 0^{\pm+}, 1^{++}, 2^{\pm+}$ . For production of  $0^{++}$  and  $2^{++}$  mesons the analysis reveals a systematic behaviour in the data that appears to distinguish between  $q\bar{q}$  and non- $q\bar{q}$  or glueball candidates. An explanation is given for the absence of  $0^{-+}$  glueball candidates in central production at present energies and the opportunity for their discovery at RHIC is noted.

---

<sup>1</sup>e-mail: F.E.Close@rl.ac.uk

The idea that glueball production might be favoured in the central region of  $pp \rightarrow pMp$  by the fusion of two Pomerons ( $\mathbb{P}$ ) is over twenty years old [1, 2]. The fact that known  $q\bar{q}$  states also are seen in this process frustrated initial hopes that such experiments would prove to be a clean glueball source. However, in [3] we noted a kinematic effect whereby known  $q\bar{q}$  states could be suppressed leaving potential glueball candidates more prominent.

Its essence was that the pattern of resonances produced in the central region of double tagged  $pp \rightarrow pMp$  depends on the vector *difference* of the transverse momentum recoil of the final state protons (even at fixed four momentum transfers). When this quantity ( $dP_T \equiv |\vec{k}_{T1} - \vec{k}_{T2}|$ ) is large, ( $\geq O(\Lambda_{QCD})$ ),  $q\bar{q}$  states are prominent whereas at small  $dP_T$  all well established  $q\bar{q}$  are observed to be suppressed while the surviving resonances include the enigmatic  $f_0(1500)$ ,  $f_0(1710)$  and  $f_0(980)$ .

The data are consistent with the hypothesis that as  $dP_T \rightarrow 0$  all bound states with internal  $L > 0$  (e.g.  $^3P_{0,2} q\bar{q}$ ) are suppressed while S-waves survive (e.g.  $0^{++}$  or  $2^{++}$  glueball made of vector gluons and the  $f_0(980)$  as any of glueball, or S-wave  $qq\bar{q}\bar{q}$  or  $K\bar{K}$  state). Models are needed to see if such a pattern is natural. Following this discovery there has been an intensive experimental programme in the last two years by the WA102 collaboration at CERN, which has produced a large and detailed set of data on both the  $dP_T$  [3] and the azimuthal angle,  $\phi$ , dependence of meson production (where  $\phi$  is the angle between the transverse momentum vectors,  $p_T$ , of the two outgoing protons).

The azimuthal dependences as a function of  $J^{PC}$  and the momentum transferred at the proton vertices,  $t$ , are very striking. As seen in refs. [4, 5], and later in this paper, the  $\phi$  distributions for mesons with  $J^{PC} = 0^{-+}$  maximise around  $90^\circ$ ,  $1^{++}$  at  $180^\circ$  and  $2^{-+}$  at  $0^\circ$ . Recently, the WA102 collaboration has confirmed that this is not simply a J-dependent effect [6] since  $0^{++}$  production peaks at  $0^\circ$  for some states whereas others are more evenly spread [7];  $2^{++}$  established  $q\bar{q}$  states peak at  $180^\circ$  whereas the  $f_2(1950)$ , whose mass may be consistent with the tensor glueball predicted in lattice QCD, peaks at  $0^\circ$  [6].

In this talk I show how these phenomena arise and in turn expose the extent to which they could be driven, at least in part, by the internal structure of the meson in question and thereby be exploited as a glueball/ $q\bar{q}$  filter [3]. We find that the  $\phi$  dependences of  $0^{-+}$  and  $1^{++}$  follow on rather general grounds if a single trajectory dominates the production mechanism. Having thus established the ability to describe the phenomena quantitatively in these cases, we predict the behaviour for  $2^{-+}$  production and then confront the  $0^{++}$  and  $2^{++}$  *glueball*/ $q\bar{q}$  sector.

To orient ourselves, think of  $e^+e^- \rightarrow e^+e^-M$  where the essential production dynamics is through  $\gamma\gamma \rightarrow M$  fusion. The photon can be polarised either  $T$  ( $\lambda = \pm 1$ ) or  $L$  ( $\lambda = 0$ ). For  $J^{PC} = 0^{++}$  the resulting structure is  $(R - \cos(\phi))^2$  where  $R$  is equal to the ratio of the

longitudinal and transverse production amplitudes for  $\gamma\gamma \rightarrow M$  and depends on the dynamical structure of the meson,  $M$ . By contrast, parity forbids the production of  $0^{-+}$  by the fusion of two scalars and also by the longitudinal (“ $L$ ”) components of two vectors. Transverse (“ $T$ ”) components are allowed and so a single amplitude drives the  $\gamma\gamma$  fusion in production of the  $0^{-+}$  states. The resulting distribution is predicted to behave like  $\sin^2(\phi)$ .

In ref. [8] it was noted that these distributions are very similar to what is found experimentally in  $pp \rightarrow pMp$  and so a CVC model for the Pomeron was used to confront the data for a range of mesons,  $M$ . The results were very similar, but not identical, to the data, e.g. the  $^3P_2$   $q\bar{q}$  states are produced dominantly with  $\lambda = 0$  in  $\mathbb{P}\mathbb{P}$  fusion instead of  $\lambda = \pm 2$  in  $\gamma\gamma$  fusion. With hindsight the reason is obvious:  $\mathbb{P}$  is not a *conserved* vector current and, in effect, has an intrinsic (and important) scalar component. One effect is that whereas amplitudes for longitudinal  $\gamma$  emission are suppressed as  $t \rightarrow 0$ , the case for the analogous  $\mathbb{P}$  grows. Suddenly everything began to fit, as summarised in ref.[9] and in the experimental paper ‘Experimental evidence for a vector-like behaviour of Pomeron exchange’ [4]. I will now show how the data can be quantitatively described in this simple picture and how characteristic features that may discriminate glueball from  $q\bar{q}$  states may ensue.

$$J^{PC} = 0^{-+}$$

The detailed calculations are described in [8, 9]. Here I shall concentrate on the  $\eta'$  meson whose production has been found to be consistent with double pomeron exchange [4]. The resulting behaviour of the cross section may be summarised as follows:

$$\frac{d\sigma}{dt_1 dt_2 d\phi'} \sim t_1 t_2 G_E^{p/2}(t_1) G_E^{p/2}(t_2) \sin^2(\phi') F^2(t_1, t_2, M^2)$$

where  $\phi'$  is the angle between the two  $pp$  scattering planes in the  $\mathbb{P}$ - $\mathbb{P}$  centre of mass and  $F(t_1, t_2, M^2)$  is the  $\mathbb{P}$ - $\mathbb{P}$ - $\eta'$  form factor. We temporarily set this equal to unity;  $pp$  elastic scattering data and/or a Donnachie Landshoff type form factor [10] can be used as model of the proton- $\mathbb{P}$  form factor ( $G_E^p(t)$ ).

The WA102 collaboration measures the azimuthal angle ( $\phi$ ) in the  $pp$  c.m. frame and so we transform the  $\phi'$  from the current c.m. frame to  $\phi$  for the  $pp$  c.m. frame. To generalise to real kinematics, we use a Monte Carlo simulation based on Galuga [11] modified for  $pp$  interactions and incorporating the  $\mathbb{P}$ -proton form factor from ref. [10].

In order to fit the data we found that the  $\mathbb{P}$ - $\mathbb{P}$ -meson form factor  $F(t_1, t_2, M^2)$  has to differ from unity. If we parametrise  $F^2(t_1, t_2, M^2)$  as  $\exp^{-b_T(t_1+t_2)}$  then we need  $b_T = 0.5 \text{ GeV}^{-2}$  in order to describe the  $t$  dependence. Fig. (1a and 1b) compare the final theoretical form for the  $\phi$  distribution and the  $t$  dependence with the data for the  $\eta'$ ; (the distributions are well

described also for the  $\eta$  but it has not yet been established that  $\mathbb{P}$ - $\mathbb{P}$  alone dominates the production of this meson).

The  $t_1 t_2$  factors in the cross section arise from the  $TT$  nature of the amplitude and will be general for the production of any  $0^{-+}$  meson. Hence for  $0^{-+}$  states with  $M \gg 1\text{GeV}$ , as expected for the lattice glueball or radial excitations of  $q\bar{q}$ , this dynamical  $t_1 t_2$  factor will suppress the region where kinematics would favour the production. It would be interesting if glueball production dynamics involved a singular  $(t_1 t_2)^{-1}$  that compensated for the transverse  $\mathbb{P}$  factor, as in this case the cross section would stand out. However, we have no reason to expect such a fortunate accident. Hence observation of high mass  $0^{-+}$  states is expected only to be favourable at extreme energies, such as at RHIC or LHC.

$$J^{PC} = 1^{++}$$

In refs. [8, 9, 12] Close and Schuler have predicted that axial mesons are produced polarised, dominantly in helicity one; this is verified by data [13]. The cross section is predicted to have the form

$$\frac{d\sigma}{dt_1 dt_2 d\phi'} \sim t_1 t_2 [\{A(t_1^T, t_2^L) - A(t_2^T, t_1^L)\}^2 + 4A(t_1^T, t_2^L)A(t_1^L, t_2^T) \sin^2(\phi'/2)]$$

where  $A(t_i, t_j)$  are the  $\mathbb{P}$ - $\mathbb{P}$ - $f_1$  form factors. In the models of refs. [9, 14] the longitudinal Pomeron amplitudes carry a factor of  $1/\sqrt{t}$  arising from the fact that, in the absence of any current conservation for the Pomeron, a longitudinal vector polarisation is not compensated. Thus we make this factor explicit and write  $A(t_i, t_j^L) = \frac{\mu}{\sqrt{t_j}} a(t_i, t_j)$ ; hence

$$\frac{d\sigma}{dt_1 dt_2 d\phi'} \sim [\{\sqrt{t_1} - \sqrt{t_2} \frac{a(t_1^T, t_2^L)}{a(t_1^L, t_2^T)}\}^2 + 4\sqrt{t_1 t_2} \frac{a(t_1^T, t_2^L)}{a(t_1^L, t_2^T)} \sin^2(\phi'/2)] a^2(t_1^L, t_2^T)$$

In the particular case where the ratio of form factors is unity, this recovers the form used in ref. [9]

$$\frac{d\sigma}{dt_1 dt_2 d\phi'} \sim [(\sqrt{t_1} - \sqrt{t_2})^2 + 4\sqrt{t_1 t_2} \sin^2(\phi'/2)] a^2(t_1, t_2)$$

which implies a dominant  $\sin^2(\phi/2)$  behaviour that tends to isotropy when suitable cuts on  $t_i$  are made. This is qualitatively realised (figs. 1e and f of ref. [4]).

We have parametrised  $a(t_i^T, t_j^L)$  as an exponential,  $\exp^{-(b_T t_i + b_L t_j)}$  where  $i, j = 1, 2$ ;  $b_T = 0.5 \text{ GeV}^{-2}$  was determined from the  $\eta'$  data above;  $b_L$  is determined from the overall  $t$  dependence

of the  $1^{++}$  production and requires  $b_L = 3 \text{ GeV}^{-2}$ . Fig. (2a and b) show the output of the model predictions from the Galuga Monte Carlo superimposed on the  $\phi$  and  $t$  distributions for the  $f_1(1285)$  from the WA102 experiment.

In addition we have a parameter free prediction of the variation of the  $\phi$  distribution as a function of  $|t_1 - t_2|$ . Fig. (2c and d) show the output of the Galuga Monte Carlo superimposed on the  $\phi$  for the  $f_1(1285)$  for  $|t_1 - t_2| \leq 0.2 \text{ GeV}^{-2}$  and  $|t_1 - t_2| \geq 0.4 \text{ GeV}^{-2}$  respectively. The agreement between the data and our prediction is excellent. Similar conclusions arise for the  $f_1(1420)$ .

$$J^{PC} = 2^{-+}$$

The  $J^{PC} = 2^{-+}$  states, the  $\eta_2(1645)$  and  $\eta_2(1870)$ , are predicted to be produced polarised. Helicity 2 is suppressed by Bose symmetry [8] and has been found to be negligible experimentally [5]. The structure of the cross section is then predicted to be

(i) helicity zero: as for the  $0^{-+}$  case,

$$\frac{d\sigma}{dt_1 dt_2 d\phi'} \sim t_1 t_2 \sin^2(\phi')$$

(ii) helicity one:

$$\frac{d\sigma}{dt_1 dt_2 d\phi'} \sim [\{\sqrt{t_1} - \sqrt{t_2} \frac{a(t_1^T, t_2^L)}{a(t_1^L, t_2^T)}\}^2 + 4\sqrt{t_1 t_2} \frac{a(t_1^T, t_2^L)}{a(t_1^L, t_2^T)} \cos^2(\phi'/2)] a^2(t_1^L, t_2^T)$$

which is as the  $1^{++}$  case except for the important and significant change from  $\sin^2(\phi'/2)$  to  $\cos^2(\phi'/2)$ .

The uncompensated factor of  $t_1 t_2$  in the helicity zero component tends to suppress this kinematically under the conditions of the WA102 experiment. Indeed, WA102 find that helicity one alone is able to describe their data [5]; this is in interesting contrast to  $\gamma\gamma \rightarrow \eta_2(Q\bar{Q})$  in the non-relativistic quark model where the helicity-one amplitude would be predicted to vanish [15]. We shall concentrate on this helicity-one amplitude henceforth.

The results of the WA102 collaboration for the  $\eta_2(1645)$  [5] are shown in fig. (3a and b). The distribution peaks as  $\phi \rightarrow 0$ , in marked contrast to the suppression in the  $1^{++}$  case (fig. 2a).

Integrating our formula over  $\phi$ , with the same approximations as previously, implies

$$\frac{d\sigma}{dt_1 dt_2} \sim (t_1 + t_2) (\exp^{-b(t_1 + t_2)})$$

and, in turn, that

$$\frac{d\sigma}{dt} \sim (1 + bt)(\exp^{-bt}) \quad (1)$$

This simple form compares remarkably well with WA102 who fit to  $\alpha e^{-b_1 t} + \beta t e^{-b_2 t}$ ; our prediction (eq. 1) implies that  $b_1 \equiv b_2$  and that  $\beta/\alpha \equiv b$  and WA102 find for the  $\eta_2(1645)$  [5]  $b_1 = 6.4 \pm 2.0$ ;  $b_2 = 7.3 \pm 1.3$  and  $\beta = 2.6 \pm 0.9$ ,  $\alpha = 0.4 \pm 0.1$

Performing the detailed comparison of model and data via Galuga, as in the previous examples, leads to the results shown in fig. (3a and b) for the  $\eta_2(1645)$ ; the  $\eta_2(1870)$  results are qualitatively similar. Bearing in mind that there are no free parameters, the agreement is remarkable. Indeed, the successful description of the  $0^{-+}$ ,  $1^{++}$  and  $2^{-+}$  sectors, both qualitatively and in detail, sets the scene for our analysis of the  $0^{++}$  and  $2^{++}$  sectors where glueballs are predicted to be present together with established  $q\bar{q}$  states. Any differences between data and this model may then be a signal for hadron structure, and potentially a filter for glue degrees of freedom.

Before turning to the  $0^{++}, 2^{++}$  channels with glueball interest, it is worth summarising exactly what we have assumed and what we have described, parameter free.

For the production of  $J^{PC} = 0^{-+}$  mesons we have predicted the  $\phi$  dependence and the vanishing cross section as  $t \rightarrow 0$  absolutely and have fitted the  $t$  slope in terms of one parameter,  $b_T$ . For the  $J^{PC} = 1^{++}$  mesons we predict the general form for the  $\phi$  distribution: it is in this channel for the first time that the non-conserved nature of the  $\mathbb{P}$  first manifests itself. The polarisation of the  $1^{++}$  is also natural. By fitting the  $t$  slope we obtain the parameter  $b_L$ ; this then gives a parameter free prediction for the variation of the  $\phi$  distribution as a function of  $t$  which agrees with the data. With parameters now fixed, we obtain absolute predictions for both the  $t$  and  $\phi$  dependences of the  $J^{PC} = 2^{-+}$  mesons which are again in accord with the data when helicity 1 dominance is imposed.

The message is that the production of the unnatural spin-parity states,  $0^{-+}, 1^{++}, 2^{-+}$ , is driven by the non-conserved vector nature of the exchanged  $\mathbb{P}$ ; it is not immediately affected by the internal structure of the produced meson. In particular, it is not sensitive to whether the mesons are glueballs or  $q\bar{q}$ .

Now I shall look at the  $0^{++}$  and  $2^{++}$  sector where glueballs are expected as well as  $q\bar{q}$ . Here we shall find that the production topologies do depend on the internal dynamics of the produced meson and as such may enable a distinction between  $q\bar{q}$  and exotic, glueball, states.

$J^{PC} = 0^{++}$  and  $2^{++}$

In contrast to the  $0^{-+}$  case, where parity forbade the LL amplitude, in the  $0^{++}$  case both  $TT$  and  $LL$  can occur. Hence there are two independent form factors [16]  $A_{TT}(t_1, t_2, M^2)$  and  $A_{LL}(t_1, t_2, M^2)$ . For  $0^{++}$  and the helicity zero amplitude of  $2^{++}$  (which experimentally is found to dominate [17]) the angular dependence of scalar meson production will be [9]

$$\frac{d\sigma}{dt_1 dt_2 d\phi'} \sim G_E^{p\ 2}(t_1) G_E^{p\ 2}(t_2) \left[ 1 + \frac{\sqrt{t_1 t_2}}{\mu^2} \frac{a_T}{a_L} e^{(b_L - b_T)(t_1 + t_2)/2} \cos(\phi') \right]^2 e^{-b_L(t_1 + t_2)} \quad (2)$$

where we have written  $a_L(t) = a_L e^{-(b_L t/2)}$  and  $a_T(t) = a_T e^{-(b_T t/2)}$  with  $b_{L,T}$  fixed to the values found earlier. The ratio  $a_T/a_L$  can be positive or negative, or in general even complex.

Eq.(2) predicts that there should be significant changes in the  $\phi$  distributions as  $t$  varies. When  $\frac{\sqrt{t_1 t_2}}{\mu^2} a_T/a_L \sim \pm 1$ , the  $\phi$  distribution will be  $\sim \cos^4(\frac{\phi}{2})$  or  $\sin^4(\frac{\phi}{2})$  depending on the sign. Indeed data on the enigmatic scalars  $f_0(980)$  and  $f_0(1500)$  show a  $\cos^4(\frac{\phi}{2})$  behaviour when  $\sqrt{t_1 t_2} \leq 0.1 \text{ GeV}^2$ , changing to  $\sim \cos^2(\phi)$  when  $\sqrt{t_1 t_2} \geq 0.3 \text{ GeV}^2$  [4].

The overall  $\phi$  dependences for the  $f_0(1370)$ ,  $f_0(1500)$ ,  $f_2(1270)$  and  $f_2(1950)$  can be described by varying the quantity  $\mu^2 a_L/a_T$ . Results are shown in fig. 4. It is clear that these  $\phi$  dependences discriminate two classes of meson in the  $0^{++}$  sector and also in the  $2^{++}$ . The  $f_0(1370)$  can be described using  $\mu^2 a_L/a_T = -0.5 \text{ GeV}^2$ , for the  $f_0(1500)$  it is  $+0.7 \text{ GeV}^2$ , for the  $f_2(1270)$  it is  $-0.4 \text{ GeV}^2$  and for the  $f_2(1950)$  it is  $+0.7 \text{ GeV}^2$ .

It is interesting to note that we can fit these  $\phi$  distributions with one parameter and it is primarily the sign of this quantity that drives the  $\phi$  dependences. Understanding the dynamical origin of this sign is now a central issue in the quest to distinguish  $q\bar{q}$  states from glueball or other exotic states.

### Acknowledgements

This is based on work performed in collaborations with A.Kirk and G.Schuler and is supported, in part, by the EU Fourth Framework Programme contract Eurodafne, FMRX-CT98-0169.

## References

- [1] D. Robson, Nucl. Phys. **B130** (1977) 328.
- [2] F.E. Close, Rep. Prog. Phys. **51** (1988) 833.
- [3] F.E. Close and A. Kirk, Phys. Lett. **B397** (1997) 333.
- [4] D. Barberis *et al.*, Phys. Lett. **B467** (1999) 165.
- [5] D. Barberis *et al.*, hep-ex/9911038 To be published in Phys. Lett.
- [6] D. Barberis *et al.*, arXiv:hep-ex/0001017 To be published in Phys. Lett.
- [7] D. Barberis *et al.*, Phys. Lett. **B462** (1999) 462.
- [8] F.E. Close and G.A. Schuler, Phys. Lett. B458 (1999) 127.
- [9] F.E. Close and G.A. Schuler, Phys. Lett. B464 (1999) 279.
- [10] A. Donnachie and P.V. Landshoff, Nucl. Phys. **B231** (1983) 189.
- [11] G.A. Schuler, Comput. Phys. Commun. **108** (1998) 279.
- [12] F.E. Close, Phys. Lett. **B419** (1998) 387.
- [13] D. Barberis *et al.*, Phys. Lett. **B440** (1998) 225; P.Chauvat, Phys.Lett. **B148** (1984) 382;  
P.Schlein, private communication.
- [14] T. Arens, O. Nachtmann, M. Diehl and P.V. Landshoff, Z. Phys **C74** (1997) 651.
- [15] F.E. Close and Zhenping Li, Z. Phys. **C54** (1992) 147.
- [16] F.E. Close, G.Farrar and Z.P.Li, Phys. Rev. **D55** (1997) 5749.
- [17] D. Barberis *et al.*, Phys. Lett. **B453** (1999) 305;  
D. Barberis *et al.*, Phys. Lett. **B453** (1999) 316.



## Figures

Figure 1: a) The  $\phi$  and b) the  $|t|$  distributions for the  $\eta'$  for the data (dots) and the model predictions from the Monte Carlo (histogram).

Figure 2: a) The  $\phi$  and b) the  $|t|$  distributions for the  $f_1(1285)$  for the data (dots) and the Monte Carlo (histogram). c) and d) the  $\phi$  distributions for  $|t_1 - t_2| \leq 0.2$  and  $|t_1 - t_2| \geq 0.4 \text{ GeV}^2$  respectively.

Figure 3: a) The  $\phi$  and b) the  $|t|$  distributions for the  $\eta_2(1645)$  for the data (dots) and the Monte Carlo (histogram).

Figure 4: The  $\phi$  distributions for the a)  $f_0(1370)$ , b)  $f_0(1500)$ , c)  $f_2(1270)$  and d)  $f_2(1950)$  for the data (dots) and the Monte Carlo (histogram).

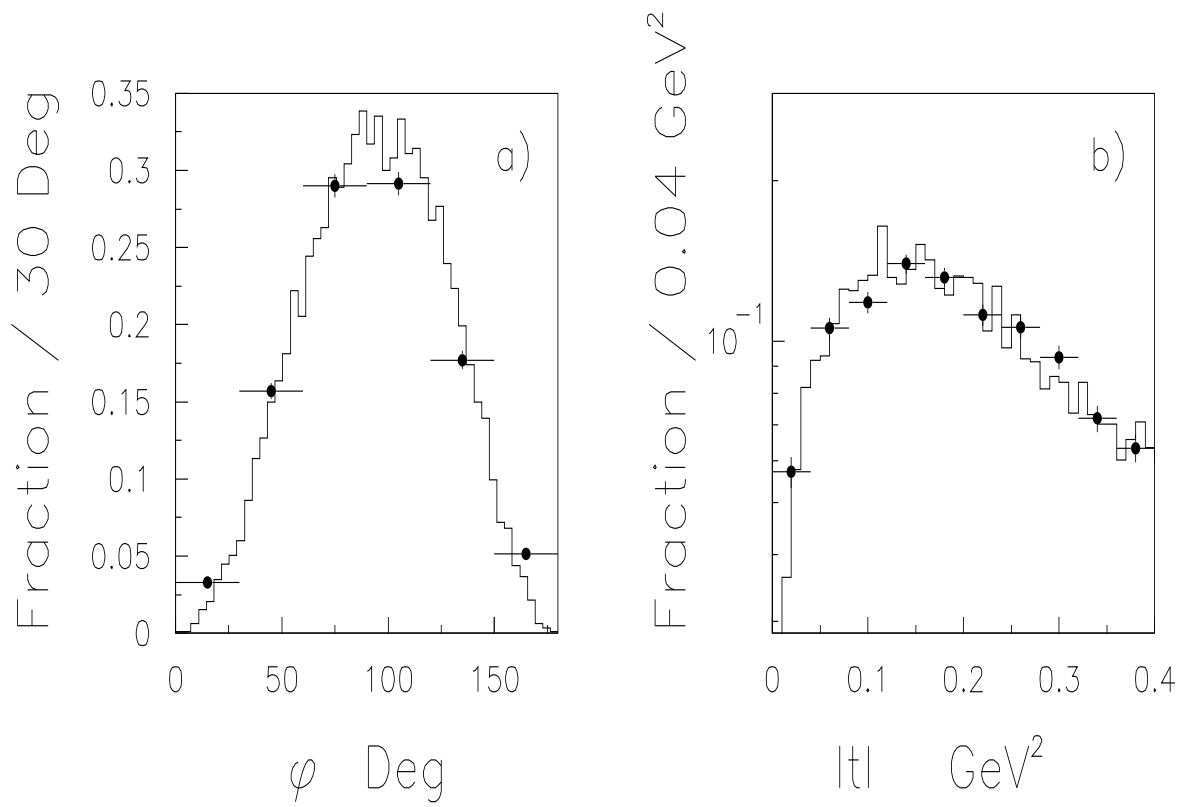


Figure 1

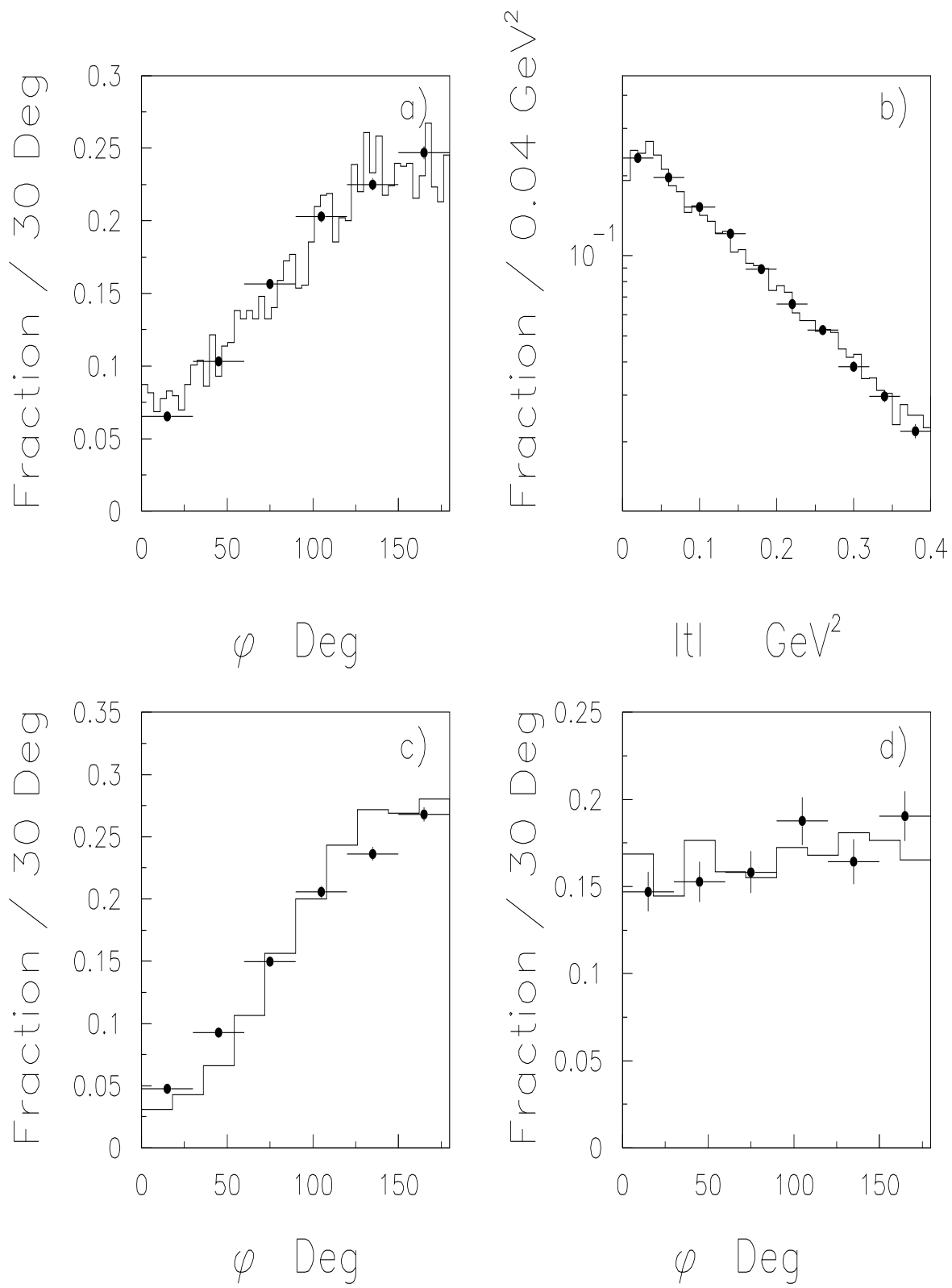


Figure 2

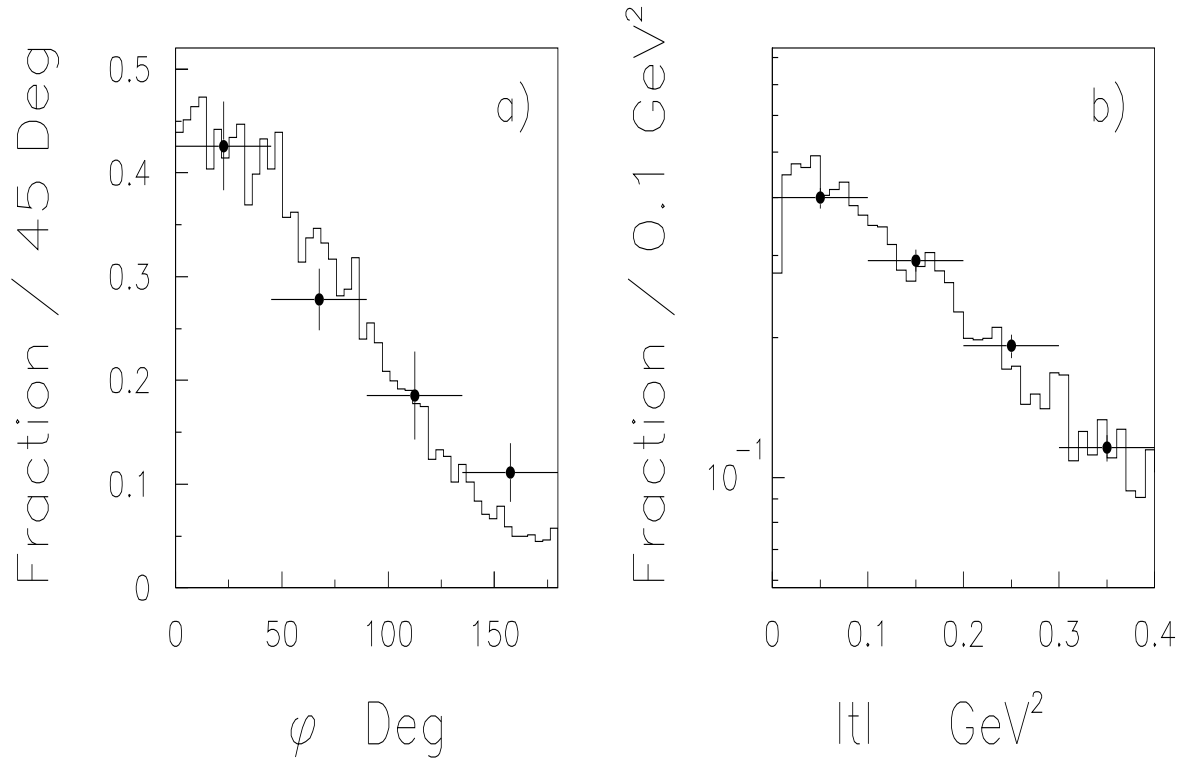


Figure 3

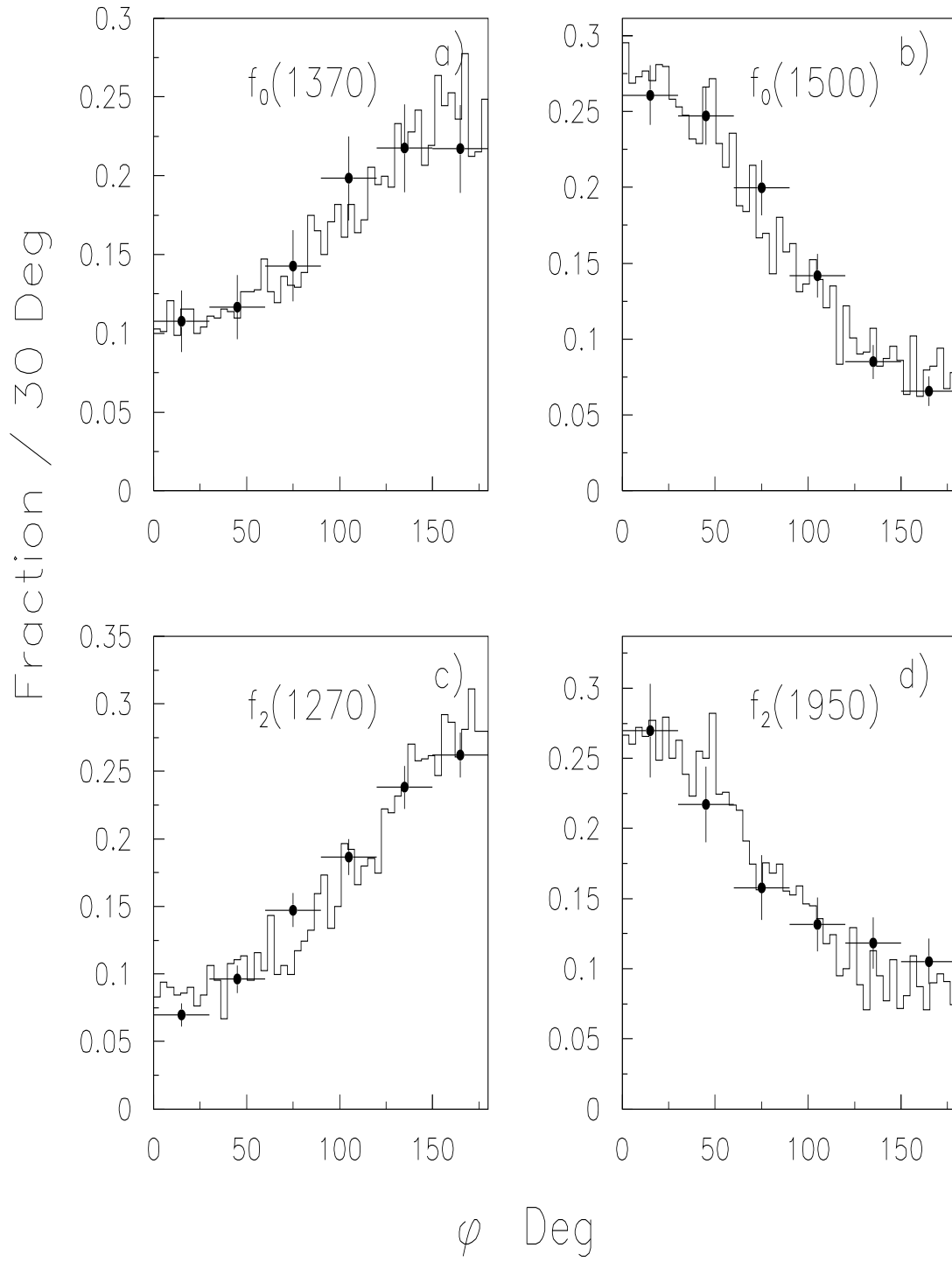


Figure 4